

Surface Orientation of 1-Methyl-, 1-Ethyl-, and 1-Butyl-3-methylimidazolium Methyl Sulfate as Probed by Sum-Frequency Generation Vibrational Spectroscopy[†]

Cherry S. Santos and Steven Baldelli*

Department of Chemistry, University of Houston, Houston, Texas 77204

Received: October 27, 2006; In Final Form: November 21, 2006

The orientation of the ions at the surface of ionic liquids has been determined by the surface-sensitive technique sum-frequency generation vibrational spectroscopy. The results indicate that both ions are present at the first layer of the gas–liquid interface. Furthermore, the alkyl chains are found to be extended toward the gas phase and away from the liquid phase. The proposed models for the preferred orientation of the ions are in good agreement in comparison with the results obtained from the recent MD simulation studies. The salts considered here are 1,3-dimethylimidazolium methylsulfate, 1-ethyl-3-methylimidazolium methylsulfate, and 1-butyl-3-methylimidazolium methylsulfate.

Introduction

Applications of room-temperature ionic liquids in a variety of relevant processes have rapidly emerged in recent years because of their unique properties. They have negligible volatility and are nonflammable with a high thermal stability and a melting point of <100 °C.¹ As a consequence, they have been used as alternatives to volatile organic solvents as media in reactions and gas-separation processes.^{2–9} In addition, since they have a relatively wide electrochemical window, they have been utilized as electrolytes in fuel cells, solar cells, and batteries.^{10–13} Given that most of these applications involve reactions at the interface, it is therefore relevant to study the structure and orientation of these ions at a molecular level to have a better understanding of their behavior. Experimental and computational studies on the structure and orientation of room temperature ionic liquids at the interface have been carried out recently by different research groups.^{14–23} Experimental studies dealt with imidazolium-based ionic liquids having a range of alkyl chain lengths paired with a number of different anions; however, the orientation and arrangement of these ions at the interface is yet to be established because the results from these studies regarding the preferred orientation of such ions vary from one technique to the other. For instance, the direct recoil spectroscopy (DRS) of [BMIM][PF₆] and [BMIM][BF₄] by Watson et al.^{18,19} showed two different surface orientations of the cations (BMIM = 1-butyl-3-methylimidazolium). The ring is oriented parallel to the surface normal with the nitrogen atoms upward, and the butyl chain is parallel to the surface plane for [BMIM][PF₆], whereas it is pointing toward the bulk liquid for the [BMIM][BF₄]. Bowers et al.¹⁴ studied the surface structure of [BMIM][BF₄] and [OMIM][PF₆] employing neutron reflectometry and suggested the lamellar structure formation for the alkyl chains. As presented in the X-ray reflectivity results of Deutsch et al.,²⁴ two molecular arrangements were proposed, one with the chain parallel to the surface plane and the other one with the chain normal to the surface plane. The models seem to be similar to the conclusion gathered from the DRS

data. These results are certainly different from the surface orientation suggested by SFG data of 1-butyl-3-methylimidazolium-based ionic liquids in dry conditions (5×10^{-5} Torr). Our previous studies indicate that the most likely orientation of the cation is such that the butyl chain is pointing toward the gas phase while the imidazolium ring is lying nearly parallel to the surface plane.^{16,17,25} Furthermore, Kim et al.²⁰ also used SFG and reported similar observation for the projection of the butyl chain for [BMIM][BF₄].

The molecular dynamics studies by Lynden-Bell²⁶ and Voth et al.²⁷ at the gas–liquid interface have yielded varying results. In the simulations performed by Lynden-Bell on 1,3-dimethylimidazolium chloride, [MMIM][Cl], she suggested that the imidazolium ring lies perpendicular to the surface with the C₂ molecular axis parallel to the interface having one CH₃ group projecting into the gas phase and the other one into the liquid phase.²⁶ This preferential orientation of [MMIM]⁺ at the gas–liquid interface is likely attributed to a high degree of alignment of the cation molecules wherein the density is believed to be enhanced.²⁶ The preferential alignment of the cation at a vertical position allows them to pack more efficiently, thus resulting in an increased density.^{22,26} On the other hand, Voth et al.²⁷ has presented a simulation on 1-ethyl-3-methylimidazolium nitrate, [EMIM][NO₃], and found that at the outermost layer of the liquid–vacuum interface, the imidazolium ring is oriented with its ring positioned parallel to the surface, whereas the ethyl group protrudes away from the surface.²⁷ This model seems to be in agreement with the SFG results for the [BMIM]⁺ cation. In addition, beneath the outermost layer there exists a dense region in which the cation orientation happens to be quite different from our suggested model. The imidazolium ring was identified to be tilting perpendicular to the surface plane with the N–CH₃ group pointing into the bulk while the ethyl group is still projected upward. Just recently, two independent simulation studies of the liquid–vapor interface based on 1-butyl-3-methylimidazolium cation were performed by Lynden-Bell et al.²⁸ and Balasubramanian et al.²⁹ Lynden-Bell et al. did the simulations on ionic liquids with [PF₆][−], [BF₄][−], and [Cl][−] anions, whereas Balasubramanian et al. considered the use of the [PF₆][−] anion. Both simulations showed that the

[†] Part of the special issue “Physical Chemistry of Ionic Liquids”.

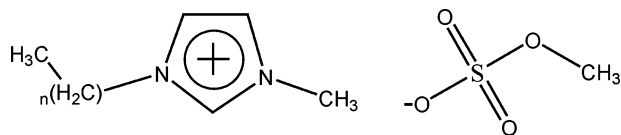


Figure 1. Structure of 1-alkyl-3-methylimidazolium methylsulfate, where n denotes the number of carbon atoms in the alkyl chain. $n = 0, 1,$ and 3 for [MMIM][MS], [EMIM][MS], and [BMIM][MS], respectively.

butyl chains are preferentially oriented along the surface normal, projecting into the vacuum phase, for all ionic liquids studied.

Our previous study on the butyl chain analog, the [BMIM]⁺ cation, at the gas–liquid interface indicates that the difference in the surface orientation is likely due to the cation structure and not the anion, since the anions, for example, [PF₆][−], [BF₄][−], [(CN)₂N][−], [I][−], do not seem to affect the cation orientation.²³ Furthermore, a recent simulation study of [BMIM][PF₆]²⁹ illustrates an interesting conclusion in which two types of molecular orientation were found to exist at the first layer of the liquid–vapor interface. This investigation offers details that might explain the differences in the surface models proposed by different groups; for instance, the contradictory findings between SFG^{16,20,25} and DRS^{18,19} experiments.

The present study includes the investigation of the surface orientation of ionic liquids 1,3-dimethylimidazolium methylsulfate, [MMIM][MS], 1-ethyl-3-methylimidazolium methylsulfate [EMIM][MS], and 1-butyl-3-methylimidazolium methylsulfate, [BMIM][MS] at the gas–liquid interface using the surface sensitive technique sum-frequency generation (SFG) vibrational spectroscopy. SFG analyses of the ionic liquids with hexafluorophosphate, [PF₆][−], as the anion were also conducted for vibration mode assignments. Figure 1 shows the general structure of the ionic liquids considered in this study. Here, the orientation at the interface of the cations, [MMIM]⁺, [EMIM]⁺, and [BMIM]⁺, and the anion, [MS][−], is evaluated as probed by SFG experiments and compared with the results of Lynden-Bell,²⁶ Voth et al.,²⁷ and Balasubramanian et al.²⁹ The SFG results suggest that the structures determined in MD simulations are correct and that the cation orientation depends on the overall imidazolium symmetry. However, the cation of [EMIM][PF₆] showed surprising results which differ from the suggested SFG orientation model for [EMIM]⁺ and [BMIM]⁺ cations. Rather, the ring may be tilted from the surface plane with the N–CH₃ group directed toward the liquid phase, but the ethyl chain is still projecting toward the gas phase. This suggests a competition between the chain–chain interaction and the Coulombic interaction between ions at the surface.

Sum-Frequency Generation. Sum-frequency generation spectroscopy has been used for these experiments due to its high surface sensitivity. It only probes molecules that are oriented at the surface; therefore, the SFG process is not allowed in the bulk liquid in which the molecules are considered to be in an isotropic environment. The theory behind the SFG process has been presented in several papers.^{30–33}

SFG is a second-order nonlinear technique that provides vibrational spectra of the molecules at interfaces. The experiment involves the spatial and temporal overlap of the tunable infrared laser and a fixed-frequency visible beam on the surface of the sample; the generated beam at the sum of the two input light fields is detected. The intensity of the emitted beam is proportional to the square of the induced polarization, $P^{(2)}$, which in turn depends on the energy of the

incoming beams, E_{IR} and E_{vis} , and the second-order nonlinear susceptibility, $\chi_{\text{eff}}^{(2)}$.

$$I(\omega_{\text{SF}}) \propto |P^{(2)}|^2 = |\chi_{\text{eff}}^{(2)} \cdot E_{\text{vis}} E_{\text{IR}}|^2 \quad (1)$$

Given that $\chi^{(2)}$ is a third-rank tensor, it vanishes in the bulk medium with inversion symmetry. Hence, there is no signal detected from the molecules in the bulk liquid state; instead, the signal only arises from the molecules at the surface where the centrosymmetry is broken. The intensity of the SFG signal is enhanced when the frequency of the infrared beam, ω_{IR} , is on resonance with the vibrational mode of the molecule. ω_n refers to the vibrational frequency, and Γ_n is the damping constant. In addition, the intensity is also dependent on the number of modes, N , and the hyperpolarizability, $\beta^{(2)}$.

$$\chi_{\text{eff}}^{(2)} = \frac{N \langle \beta^{(2)} \rangle}{\omega_{\text{IR}} - \omega_n + i\Gamma_n} \quad (2)$$

$\beta^{(2)}$ contains contributions from the Raman polarizability and IR dipole transition of the molecule, which indicates that all resonances in SFG spectroscopy must be both infrared and Raman-active and are orientationally averaged as indicated by the angled brackets, $\langle \rangle$.

In this paper, the interest is directed to the C–H stretching modes of the methyl group attached to the nitrogen atom of the [MMIM]⁺ cation and from the alkyl chain of the [EMIM]⁺ and [BMIM]⁺, as well as the methyl group of the methylsulfate anion. The methyl group is assumed to have C_{3v} symmetry with a free rotation about the C_3 axis. The molecular orientation, tilt angle, θ , of the methyl group is determined with respect to the surface normal. Polarization null angle (PNA) measurements were employed for the orientation determination.^{34–36}

Experimental Section

Sample Preparation. The samples were synthesized using a previously published procedure.³⁷ All chemicals were purchased from Sigma-Aldrich and used as received, except for 1-butylimidazole, which was distilled prior to use. Samples were characterized using ¹H–NMR and IR spectroscopy.

[MMIM][MS], [EMIM][MS], and [BMIM][MS]. The synthesis of an ionic liquid with a methylsulfate anion involved the alkylation of 1-alkylimidazole with dimethylsulfate in toluene. Dimethylsulfate was added dropwise into the mixture of 1-alkylimidazole and toluene maintaining the temperature of the solution below 40 °C. The reaction was kept under nitrogen until completed. The lower ionic liquid phase was washed with toluene (3×) and dried with heating (~70 °C) under vacuum. Liquid samples were clear and colorless after purification using activated charcoal.

[MMIM][PF₆] and [EMIM][PF₆]. Both samples were prepared by the metathesis of [MMIM][MS] and [EMIM][MS] with hexafluorophosphoric acid, HPF₆. The acid was added to a solution of the corresponding ionic liquid and water with stirring, followed by the addition of aqueous sodium hydroxide. Formation of a white precipitate was evident upon cooling in an ice bath. The white, solid product was collected by filtration.

The spectroscopy cell used for the experiments was made entirely of glass with Teflon stopcocks, Kalrez O-rings, and IR quartz windows. The cell was cleaned with 50/50 HNO₃/H₂SO₄ solution, followed by repeated rinsing with deionized water from a Millipore A10 system (>18 MΩ·cm), and dried in a vacuum line before being filled with the sample. Prior to conducting the SFG experiment, each sample was transferred

to the cleaned spectroscopy cell and dried in a vacuum line, with stirring and heating at ~ 60 °C, except for [MMIM][PF₆] (temperature at ~ 90 °C), until it reached a pressure of 5×10^{-5} Torr. The water content is determined by Henry's law using the values previously established by Brennecke³⁸ and estimated to be 1.2×10^{-6} mol fraction. The cell was backfilled with argon gas, ≥ 2 atm before being removed from the vacuum line.

SFG Spectroscopy. The details of the optical setup have been described in previous papers.^{16,23} The SFG experiment was conducted following a procedure similar to that described previously.^{16,23} The SFG spectra of all the ionic liquids were acquired at room temperature, except for [MMIM][PF₆] and [EMIM][PF₆], which were acquired at 90 and 70 °C, respectively. The high melting salts were heated using a heating plate, and a type-K thermocouple in a glass sleeve inserted into the cell was used to monitor the temperature directly from the ionic liquid. The data presented here were averages of five scans with error bars representing the standard deviation among the spectra. The data were collected using an infrared frequency scan rate of $1 \text{ cm}^{-1}/\text{s}$ and 20 shots/point. Each spectrum was corrected for IR fluctuations and normalized relative to the *ssp* (*s*-polarized SFG beam, *s*-polarized visible light, and *p*-polarized IR beam) spectrum of the CH₃ symmetric stretch peak. The fitting of SFG spectra was carried out using Origin 7.0 Professional nonlinear curve fitting. Equation 2 was used as the fitting function, and the instrumental weighting method was applied.

Results

The SFG spectra of the methylsulfate-based ionic liquids showed the presence of C–H stretching mode vibrations from both the cation and anion. Both [EMIM][MS] and [BMIM][MS] salts display similar features, except for the relative peak intensities, whereas the [MMIM][MS] showed entirely different spectral features for its cation when compared with the other two compounds. On the other hand, all three hexafluorophosphate-based samples exhibited different spectra relative to one other.

Peak Assignment. SFG spectra of methylsulfate ionic liquids for four polarization combinations (*ssp*, *ppp*, *sps*, and *pss*) are given in Figure 2, and the *ssp* and *ppp* spectra for [PF₆][−] ionic liquids are shown in Figure 3. Since peaks were not observed in the *sps* and *pss* spectra of [PF₆][−] ionic liquids, they are not shown here. Tables 1–3 show the vibration mode assignments and their corresponding frequencies. Peak assignments are based on Raman and infrared spectroscopy of 1-methylimidazole^{39,40} for the imidazolium ring and *n*-alkyl chains⁴¹ for the butyl and ethyl chains, and SFG and Raman studies on methanol^{36,42–44} for the methylsulfate anion.

[MMIM][MS]. There are three discernible peaks in the 2750–3000 cm^{-1} region of the *ssp* polarization spectrum. The peaks are accounted for with four vibrations that are due to the C–H vibration modes from the two different methyl groups, the N–CH₃ on the [MMIM]⁺ cation and the O–CH₃ from the methylsulfate anion. The *ssp* spectrum (Figure 2A) shows vibrations at ~ 2827 and $\sim 2905 \text{ cm}^{-1}$ that can be assigned to the O–CH₃ symmetric stretch and its Fermi resonance, whereas the intense peak at $\sim 2953 \text{ cm}^{-1}$ has contributions from both N–CH₃ symmetric and O–CH₃ antisymmetric vibrations.^{23,36,39,40,43} The assignment of the O–CH₃ antisymmetric mode here is not in accord with the previous SFG studies on methanol in which they attributed the peak at $\sim 2953 \text{ cm}^{-1}$ to another Fermi resonance in addition to the $\sim 2905 \text{ cm}^{-1}$ peak.^{36,42–44} However, the O–CH₃ antisymmetric assignment

agrees well with the DFT calculation performed on the C–H stretching vibrations of [MMIM][MS] by Lin et al.⁴⁵ They have assigned two modes at 2876 and 2948 cm^{-1} to the symmetric and antisymmetric vibrations, respectively, of the O–CH₃ group. The C–H antisymmetric mode of the O–CH₃ group observed in the *ssp* spectrum is further confirmed in the *ppp*, *sps*, and *pss* spectra, which show at $\sim 2970 \text{ cm}^{-1}$ (Figure 2B–D).

The antisymmetric mode of N–CH₃ group is observed at $\sim 3000 \text{ cm}^{-1}$ in the *ppp* spectrum, as well as in the *sps* and *pss* spectra (Figure 2B–D).^{23,39,40} In addition, from the DFT calculation performed by Lin et al.,⁴⁵ the vibrations at 2954 and 3034–3048 cm^{-1} were assigned to the symmetric and antisymmetric vibrations, respectively, of this group. They have also carried out an IR study that exhibited three bands at 2953, 3114, and 3161 cm^{-1} , which were all assigned to the C–H stretching modes of the cation. The band at 2953 cm^{-1} has been attributed to the stretching mode of the methyl group, and both 3114 and 3161 cm^{-1} bands were due to the imidazolium ring vibrations. The assigned peak positions here for both methyl groups of [MMIM][MS] coincide very well with the DFT calculation and the IR study of Lin et al.⁴⁵ In addition, IR and Raman experiments performed on the deuterated sample of [BMIM]-[PF₆] confirmed that N–CH₃ symmetric and antisymmetric modes were observed at 2968 and 3035 cm^{-1} .²³ Furthermore, the peak at $\sim 2905 \text{ cm}^{-1}$ as assigned to the Fermi resonance of the methyl group from the anion has been verified by the characterization of [MMIM][PF₆].

Figure 3 displays the spectra of the [MMIM][PF₆]. In this case, only C–H vibrations from the cation would be observed, and any contributions from the anion have been eliminated. As it turned out, the salt does not exhibit any vibration at $\sim 2905 \text{ cm}^{-1}$; hence, this peak comes from the methylsulfate anion.^{36,43} Only one resonance is observed in the *ssp* spectrum which is at $\sim 2965 \text{ cm}^{-1}$, and this has been assigned as the N–CH₃ symmetric mode.^{23,39,40} Both [MMIM][MS] and [MMIM][PF₆] do not exhibit vibrations from the ring modes.

[EMIM][MS]. The SFG spectra of the [EMIM][MS] (Figure 2E–H) look similar to the [MMIM][MS], except for the extra mode at 2878 cm^{-1} in the *ssp* spectrum, and are due to the CH₃ group of the ethyl chain. Three different methyl groups are present in this compound, but the observed vibrations come only from the methyl groups of the ethyl chain and the methylsulfate anion. There is no vibration observed from the N–CH₃ of the [EMIM]⁺ cation, which is in contrast to the spectra of [MMIM][MS]. The mode assignments for the methylsulfate anion are analogous to the [MMIM][MS], but the peak assignments for the [EMIM]⁺ cation are different from the [MMIM]⁺ cation. The mode at $\sim 2878 \text{ cm}^{-1}$ comes from the symmetric methyl stretch of the ethyl chain (C–CH₃), whereas the peak at $\sim 2952 \text{ cm}^{-1}$ has contributions from both the C–CH₃ Fermi resonance and the O–CH₃ antisymmetric stretch.^{23,36,40,41,43} The *ppp* spectrum shows two peaks at ~ 2959 and $\sim 2980 \text{ cm}^{-1}$, which are assigned to the antisymmetric modes of C–CH₃ and O–CH₃, respectively.^{41,43} The SFG spectra of [EMIM][PF₆] (Figure 3) display peaks that are significantly different from those of the [EMIM][MS]. In this instance, the *ssp* spectrum shows vibrations at ~ 2884 , ~ 2947 , ~ 2970 , and $\sim 3180 \text{ cm}^{-1}$, which correspond to the C–CH₃ symmetric; both C–CH₃ Fermi resonance and N–CH₂ symmetric; N–CH₃ symmetric; and the H–C(4)–C(5)–H symmetric vibrations of the imidazolium ring, respectively.^{23,39–41,45,46} The N–CH₂ symmetric mode ($\sim 2947 \text{ cm}^{-1}$) has been assigned according to the Raman study of [EMIM][PF₆] by Talaty et al.,⁴⁶ in which their study showed that this vibration was

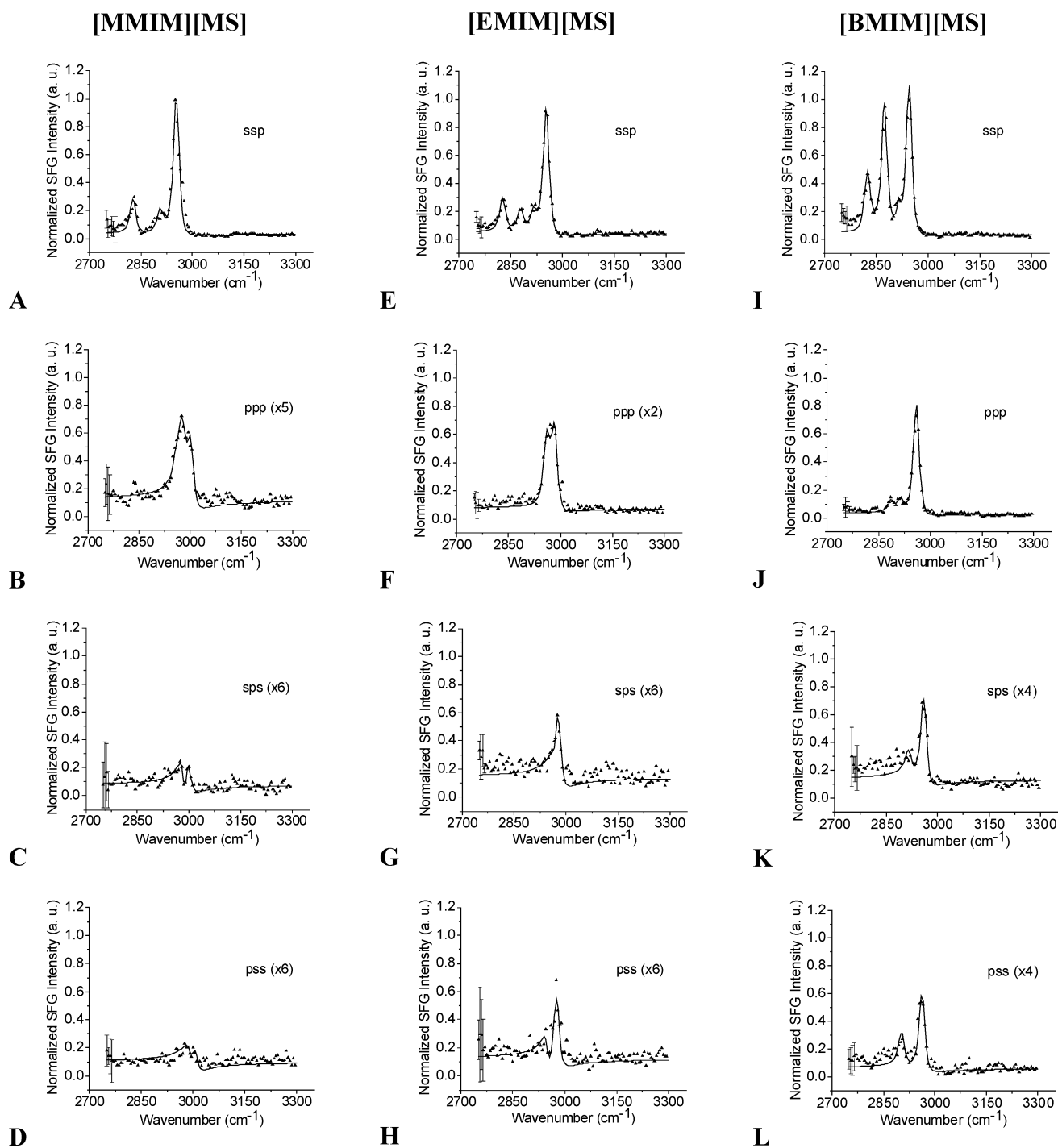


Figure 2. SFG spectra of [MMIM][MS] (A–D), [EMIM][MS] (E–H), and [BMIM][MS] (I–L) for four polarization combinations.

observed at 2942 cm^{-1} . Conversely, the features at ~ 2960 and $\sim 2988\text{ cm}^{-1}$ in the *ppp* spectrum are attributed to the antisymmetric stretches of C–CH₃ and N–CH₃, respectively.^{23,39–41}

[BMIM][MS]. The *ssp* spectrum of [BMIM][MS] (Figure 2I) shows four distinct modes in the aliphatic C–H region of the spectrum. The spectral features are similar to the [EMIM][MS], except for the relative peak intensities. Resonances due to the O–CH₃ group, the symmetric stretch and Fermi resonance, at ~ 2827 and $\sim 2915\text{ cm}^{-1}$, respectively, and C–CH₃ symmetric stretch at $\sim 2878\text{ cm}^{-1}$ and its Fermi resonance at $\sim 2945\text{ cm}^{-1}$ are observed.^{23,36,41,43} The $\sim 2945\text{ cm}^{-1}$ mode however, is noticed to be more intense than the C–CH₃ symmetric peak ($\sim 2878\text{ cm}^{-1}$). As reported previously, the *ssp* spectrum of [BMIM][PF₆] showed a significantly less intense

peak at $\sim 2945\text{ cm}^{-1}$, where $A_{\text{CH}_3(\text{sym})}/A_{\text{CH}_3(\text{FR})} = 1.5$.^{16,17,23} In this particular case, the anion in [BMIM][PF₆] does not have any C–H vibrations; hence, the O–CH₃ contribution has been eliminated. Therefore, it is believed that the remaining intensity from the $\sim 2945\text{-cm}^{-1}$ peak is due to the CH₃ group of the methylsulfate anion. The added intensity cannot be solely attributed to the Fermi resonance of the O–CH₃ symmetric stretch (see Figure 2I and ref 15: Figure 5A). Instead, the O–CH₃ antisymmetric mode has also some contributions to the $\sim 2945\text{ cm}^{-1}$ peak, as in the case of [MMIM][MS] and [EMIM][MS]. In the *ppp* spectrum of [BMIM][MS], the strong antisymmetric stretch at $\sim 2970\text{ cm}^{-1}$ belongs to the methyl group at the end of the butyl chain.⁴¹ The same vibrational mode is observed in both *sps* and *pss* spectra. However, unlike in the

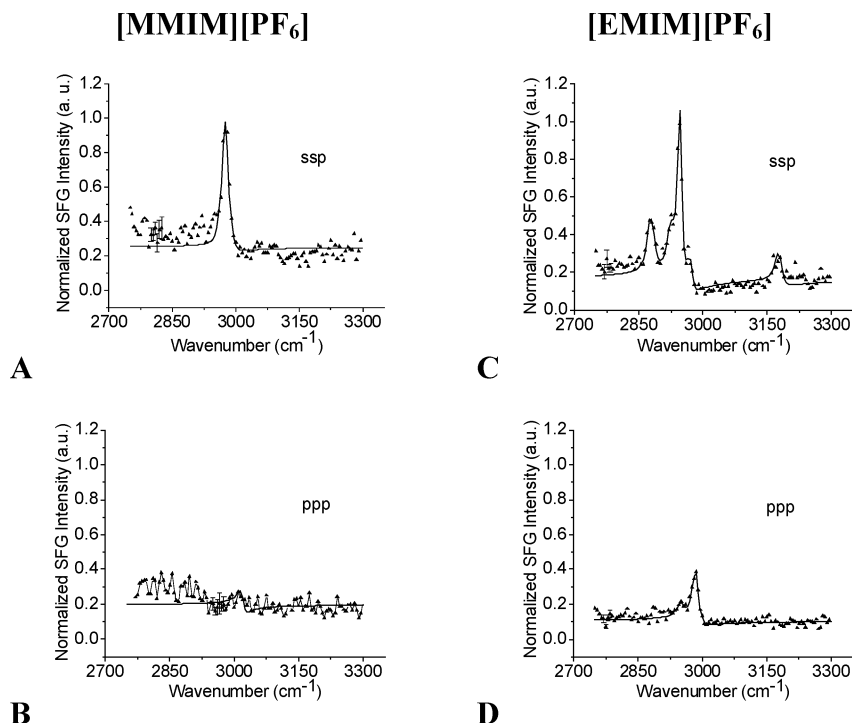


Figure 3. SFG spectra of [MMIM][PF₆] (A, B) and [EMIM][PF₆] (C, D) for *ssp* and *ppp* polarization combinations.

TABLE 1: C–H Stretching Mode Assignments for [MMIM][MS] and [MMIM][PF₆]

assignment	frequency (cm ⁻¹)	
	[MMIM][MS]	[MMIM][PF ₆]
O–CH ₃ (sym) ^{36,43,45}	2827	
O–CH ₃ (FR) ^{36,43,45}	2905	
O–CH ₃ (asym) ^{36,43,45}	2970	
N–CH ₃ (sym) ^{23,39,40}	2953	2965
N–CH ₃ (asym) ^{23,39,40}	3000	

TABLE 2: C–H Stretching Mode Assignments for [EMIM][MS] and [EMIM][PF₆]

assignment	frequency (cm ⁻¹)	
	[EMIM][MS]	[EMIM][PF ₆]
O–CH ₃ (sym) ^{36,43,45}	2827	
O–CH ₃ (FR) ^{36,43,45}	2915	
O–CH ₃ (asym) ^{36,43,45}	2980	
C–CH ₃ (sym) ^{23,40,41}	2878	2884
C–CH ₃ (FR) ^{23,40,41}	2952	2947
C–CH ₃ (asym) ^{23,40,41}	2959	2960
N–CH ₂ (sym) ⁴⁶		2947
N–CH ₃ (sym) ^{23,39,40}		2970
N–CH ₃ (asym) ^{23,39,40}		2988
H–C(4)–C(5)–H (sym) ³⁹		3180

TABLE 3: C–H Stretching Mode Assignments for [BMIM][MS] and [BMIM][PF₆]

assignment	frequency (cm ⁻¹)	
	[BMIM][MS]	[BMIM][PF ₆] ^{16,23}
O–CH ₃ (sym) ^{36,43,45}	2827	
O–CH ₃ (FR) ^{36,43,45}	2915	
C–CH ₃ (sym) ^{23,40,41}	2878	2880
C–CH ₃ (FR) ^{23,40,41}	2945	2950
C–CH ₃ (asym) ^{23,40,41}	2970	2970

[MMIM][MS] and [EMIM][MS], the O–CH₃ antisymmetric mode is not clearly visible in the *ppp* spectrum. In addition, there are no resonances observed from the imidazolium ring or N–CH₃ group in any of the four polarization spectra.

Appearance of all mentioned vibrational modes indicates that these are the groups that are present and oriented at the interface, since SFG only probes molecules at the surface that have a net polar orientation.⁴⁷ Consequently, the results suggest that both cation and anion are present at the gas–liquid interface. There are no features in the spectra that are due to the C–H vibrational modes of the imidazolium ring at ~ 3150 cm⁻¹ and ~ 3175 cm⁻¹ for H–C(4)–C(5)–H, being the symmetric and antisymmetric stretches, respectively, and at ~ 3020 cm⁻¹ for C(2)–H symmetric, for all ionic liquids studied here, except for the [EMIM][PF₆].³⁹ However, in contrast to [MMIM][MS], a vibrational mode from N–CH₃ is not observed for [EMIM][MS] and [BMIM][MS]. This suggests a completely different orientation for the symmetric cation, [MMIM]⁺.

PNA Measurements. The null angle (Ω_{null}) measurements for the symmetric stretch vibration of the methyl group from the ring and the methylsulfate anion of the [MMIM][MS] are presented in Figures 4A and 5A, respectively. The minimum from the curve is observed at $+15^\circ$ for N–CH₃ and $+0.5^\circ$ for the O–CH₃. Figures 4B and 5B show the theoretical plots of the polarization null angle for [MMIM][MS]. The average tilt angle is given by the minimum in the polarization curve. PNA measurements were also performed on [EMIM][MS], but the analysis of the data offered inaccurate results due to the weak intensity of the CH₃ symmetric stretch peak; hence, they are not reported. The PNA results for [BMIM][MS] were presented elsewhere.⁴⁸ The measurements for the symmetric stretch mode of the methyl group from the butyl chain and the methylsulfate anion gave the minimum of $10 \pm 2^\circ$ and $2 \pm 3^\circ$, respectively.

Discussion

Orientation Analysis. The orientation analysis of the methyl groups from the methylsulfate, 1,3-dimethylimidazolium cation, and the butyl chain of 1-butyl-3-methylimidazolium cation was performed using polarization null angle measurements as outlined by Wang et al.^{34,35,49}

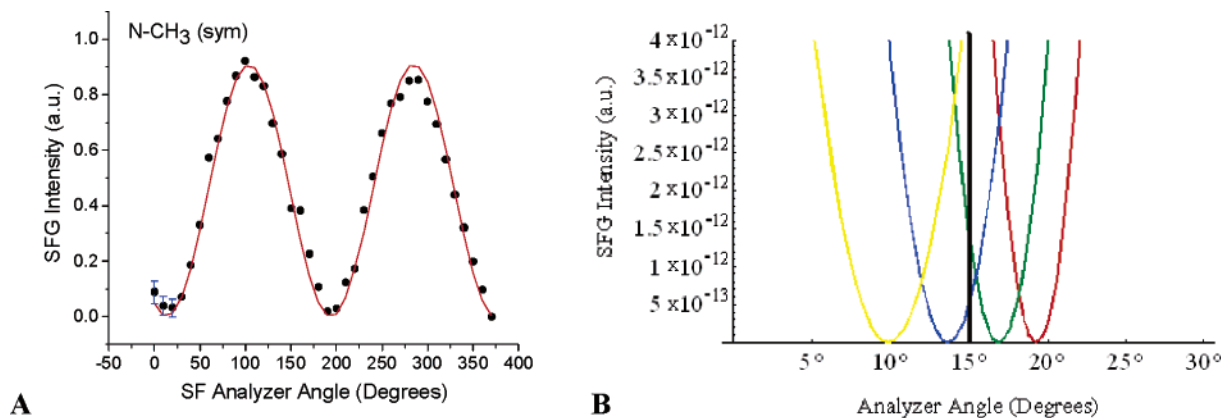


Figure 4. (A) Measured null angle for N-CH₃ (sym) on the imidazolium ring. (B) Theoretical curves for null angle analysis red → yellow are for tilt angle 20 → 50°, Δ10°. Measured null angle is 15°, which corresponds to a tilt angle of 35°. Vertical line indicates measured null angle.

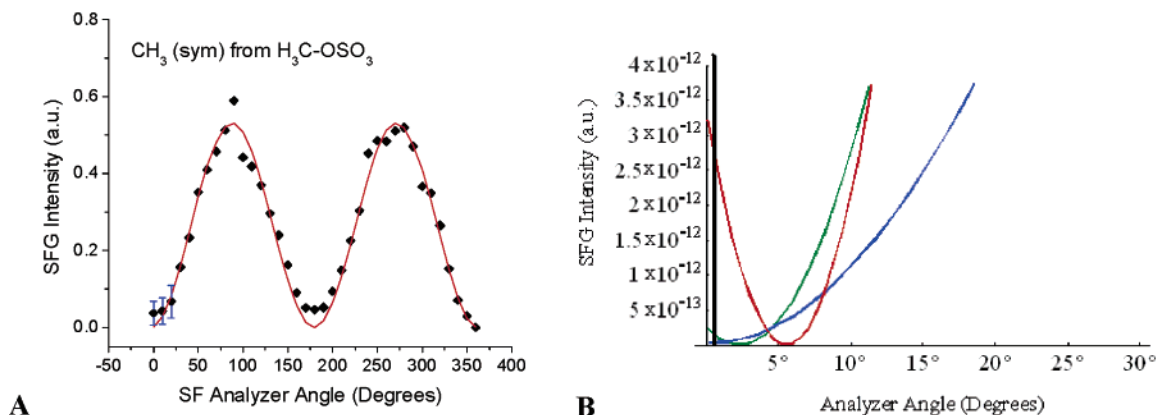


Figure 5. (A) Polarization curve for methylsulfate anion CH₃(sym). (B) Theoretical curves for null angle analysis red → blue are for tilt angles 60° → 80°, Δ10°. The measured null angle is 0.5° which corresponds to a tilt angle of 75°. Vertical line indicates the measured null angle.

The SFG signal is proportional to the square of the effective susceptibility, $I_{\text{SF}} \propto |\chi_{\text{eff}}^{(2)}|^2$.

$$\begin{aligned} \chi_{\text{eff}}^{(2)} = & \sin \Omega_{\text{sf}} \sin \Omega_{\text{vis}} \cos \Omega_{\text{IR}} L_{\text{yy, sf}} L_{\text{yy, vis}} L_{\text{zz, IR}} \sin \beta_{\text{IR}} \chi_{\text{yyz}} \\ & + \sin \Omega_{\text{sf}} \cos \Omega_{\text{vis}} \sin \Omega_{\text{IR}} L_{\text{yy, sf}} L_{\text{zz, vis}} L_{\text{yy, IR}} \sin \beta_{\text{vis}} \chi_{\text{zyz}} \\ & + \cos \Omega_{\text{sf}} \sin \Omega_{\text{vis}} \sin \Omega_{\text{IR}} L_{\text{zz, sf}} L_{\text{yy, vis}} L_{\text{yy, IR}} \sin \beta_{\text{sf}} \chi_{\text{zyz}} \\ & - \cos \Omega_{\text{sf}} \cos \Omega_{\text{vis}} \cos \Omega_{\text{IR}} L_{\text{xx, sf}} L_{\text{xx, vis}} L_{\text{zz, IR}} \cos \beta_{\text{sf}} \\ & \quad \cos \beta_{\text{vis}} \sin \beta_{\text{IR}} \chi_{\text{xxz}} - \cos \Omega_{\text{sf}} \cos \Omega_{\text{vis}} \\ & \quad \cos \Omega_{\text{IR}} L_{\text{xx, sf}} L_{\text{zz, vis}} L_{\text{xx, IR}} \cos \beta_{\text{sf}} \sin \beta_{\text{vis}} \cos \beta_{\text{IR}} \chi_{\text{xxz}} \\ & + \cos \Omega_{\text{sf}} \cos \Omega_{\text{vis}} \cos \Omega_{\text{IR}} L_{\text{zz, sf}} L_{\text{xx, vis}} L_{\text{xx, IR}} \sin \beta_{\text{sf}} \cos \beta_{\text{vis}} \\ & \quad \cos \beta_{\text{IR}} \chi_{\text{zxx}} + \cos \Omega_{\text{sf}} \cos \Omega_{\text{vis}} \cos \Omega_{\text{IR}} L_{\text{zz, sf}} L_{\text{zz, vis}} L_{\text{zz, IR}} \sin \\ & \quad \beta_{\text{sf}} \sin \beta_{\text{vis}} \sin \beta_{\text{IR}} \chi_{\text{zzz}} \end{aligned}$$

The surface is considered isotropic in the x - y surface plane; therefore, the following relations among the surface susceptibilities are made.

$$\chi_{\text{xxz}}^{(2)} = \chi_{\text{xxz}'}^{(2)}, \quad \chi_{\text{zxx}}^{(2)} = \chi_{\text{zyz}}^{(2)}, \quad \chi_{\text{zxx}}^{(2)} = \chi_{\text{zyy}}^{(2)}, \quad \chi_{\text{zzz}}^{(2)}$$

The effective second-order susceptibility, $\chi_{\text{eff}}^{(2)}$, contains all the information on the orientation of surface molecules, whereas $\chi^{(2)}$, a third-rank tensor, refers to the macroscopic second-order nonlinear susceptibility. The polarization angle for the optical electric fields is represented as Ω_i , and β_i denotes the angle of the input laser beams relative to the surface normal with the corresponding frequency, i . L_{ii} represents the Fresnel coefficient of the three laser beams.

The methyl group is approximated as C_{3v} symmetry; thus, the hyperpolarizabilities are related when the sum frequency and visible beam are not at resonance with the molecule.

$$\begin{aligned} \beta_{aac} = \beta_{bbc}, \quad \beta_{ccc}, \quad \beta_{aca} = \beta_{bcb} = \beta_{cbb} = \beta_{caa}, \quad \beta_{aaa} = -\beta_{bba} = \\ -\beta_{abb} = -\beta_{bab} \end{aligned}$$

Values for the hyperpolarizability are derived from the bond additivity model in which bond polarizability is $r = \alpha_{aa}/\alpha_{cc} = 0.28$ for the CH₃ group of the methylsulfate anion. The method to relate bond polarizability (α_{ij}) to group or molecular hyperpolarizability (β_{ijk}) has been thoroughly presented by others.^{47,49–54}

[MMIM][MS]. The measured null angle (Ω_{null}) for the CH₃ symmetric stretch of [MMIM]⁺ is +15°, which gives a tilt angle of ~35° from the surface normal for the C_3 axis, as shown in Figure 4B. This value is sensitive to the bond polarizability and is illustrated in Figure 6. For $r = 0.1$ – 0.5 , the tilt angle varies from 17° to 43° at the measured null angle of +15°. A value of $r = 0.28$ is used for the analysis based on previous work for the CH₃ group connected to a heteroatom.⁴⁹ Typically, $r = 0$ – 0.03 for a CH₃ group in an aliphatic chain.^{49,52–54} The polarization null angle on the methylsulfate anion is shown in Figure 5B. The measured null angle is +0.5°, which results in tilt angles ranging from 65 to 75° from the surface normal. All the orientations mentioned in this study refer to the averages over a distribution of oriented molecules in the neat liquid.

The presence of C–H modes from the N-CH₃ group in the case of [MMIM][MS] is an indication that the cation is polar oriented with one methyl group protruding out of the surface,

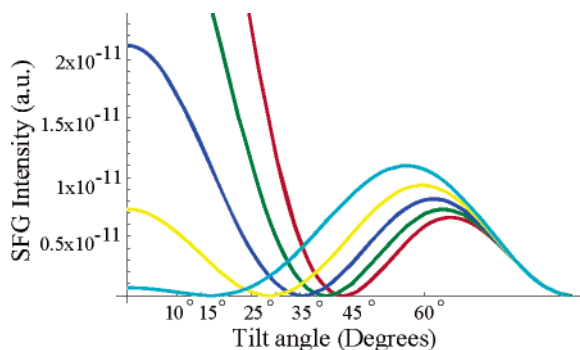


Figure 6. Polarization null angle plots for $r = 0.1–0.5$ (red \rightarrow cyan). $\Omega_{\text{null}} = 15^\circ$.

and the molecular plane is parallel to the surface normal or vertically aligned at the surface. The orientation also shows that the C_2 axis is approximately parallel to the surface plane. This is further supported by the PNA analysis, which shows that CH_3 group has a tilt angle of $\sim 35^\circ$ from the surface normal and is consistent with the model of Lynden-Bell.²⁶ In her simulation, she found a significant degree of orientational ordering of the cation near the surface. According to Lynden-Bell, the orientational preference of the cation at the surface could be attributed to the fact that this alignment would allow them to pack more closely, which then results in an increased density.²⁶ In addition, this close packing is supported by the formation of hydrogen bonds observed in the single-crystal X-ray structure of pure 1,3-dimethylimidazolium methylsulfate determined by Holbrey et al.³⁷ From their investigation, the hydrogen bond is formed between the hydrogen atoms of C(2), C(4), and C(5) and the terminal oxygen atoms of the methylsulfate anion.

However, this orientation appears to be specific for $[\text{MMIM}]^+$ and has not been observed in any of the butylimidazolium-based ionic liquids studied using the SFG technique at the gas–liquid interface.^{16,17,20,23,55} The CH_3 symmetric mode of the methylsulfate, on the other hand, gave a tilt angle of $65–70^\circ$, which is tipped significantly at the surface.

This distinct orientation of the $[\text{MMIM}]^+$ cation is interesting to compare with a cation that has a relatively longer chain attached to one of the nitrogen atoms to find out if decreasing the symmetry of the cation and increasing the chain–chain interactions would give a considerably different orientation at the surface.

[EMIM][MS] and [BMIM][MS]. Consequently, the increase in the chain length of the alkyl substituent on the cation seems to have a significant influence on the ring orientation of both compounds, [EMIM][MS] and [BMIM][MS]. Because SFG probes only the vibrations with polar ordering, the absence of the C–H modes from N– CH_3 , C(2)–H, and H–C(4)–C(5)–H of the imidazolium ring suggests that the dipole transition is projected parallel to the surface plane in the case of these two compounds. Hence, for both salts, the ring orientation is taken to be parallel to the surface plane. The previous SFG studies performed on imidazolium-based ionic liquids with a butyl chain substituent paired with different anions showed a ring orientation similar to that of the $[\text{BMIM}]^+$ in $[\text{BMIM}][\text{MS}]$.^{16,17,23,48} A further confirmation on the ring orientation is the SFG study on the deuterated $[\text{BMIM}][\text{PF}_6]$.²³ The study showed that the absence of the modes from the N– CH_3 group is due to the orientation of the imidazolium ring and not on any interference with either symmetric mode or Fermi resonance of the CH_3 group at the end of the butyl chain. Furthermore, the dominance in the *ssp* spectra over other polarization combinations of the symmetric stretch and the Fermi resonance peaks of the CH_3

group at the end of the ethyl and butyl chains means that the methyl group has an average orientation pointing upward. In fact, a recent study on $[\text{BMIM}][\text{MS}]$ employing SFG and X-ray crystallography verified this conclusion.⁴⁸ A phase simulation performed on the methyl groups of the butyl chain and the anion showed clearly that both methyl groups were pointing upward. Moreover, crystallographic evidence confirmed that the butyl chain has an all-trans conformation, and both ions were located adjacent to one another.⁴⁸ In addition, SFG studies on ionic liquid–water mixtures showed the surfactant-like behavior of these salts.^{16,17,25,55} The net ordering at the surface of imidazolium salts can be understood as a result of placing the hydrophobic alkyl group toward the vapor phase to maximize the interaction between ions near the surface, which then minimizes the surface energy. The projection of the chain toward the gas phase is consistent with the concept that the functional groups with a low surface energy are present at the surface, which in this instance is the alkyl group.^{56–58} A similar orientation of the butyl chain has been noted in SFG studies of $[\text{BMIM}][\text{BF}_4]$ and $[\text{BMIM}][\text{PF}_6]$ by Kim et al.²⁰ An earlier study on $[\text{EMIM}][\text{TF}_2\text{N}]$ utilizing electron spectroscopy techniques, metastable impact electron spectroscopy (MEIS) in combination with ultraviolet photoelectron spectroscopy (UPS), and X-ray photoelectron spectroscopy (XPS) found that both cation and anion are present at the surface layer.^{59,60} Apparently, the ethyl group has been determined to be directed toward the vacuum, which further supports the conclusion suggested for the projection of the butyl chain of the butylimidazolium salts utilizing the SFG technique. Even as a result of the simulation calculations of Del Popolo et al.,²⁸ a similar conformation for butyl chains on 1-butyl-3-methylimidazolium $[\text{PF}_6]^-$, $[\text{BF}_4]^-$, and $[\text{Cl}]^-$ ionic liquids was proposed.

Orientation analysis of $[\text{BMIM}][\text{MS}]$ that is based on polarization null angle measurements of $[\text{BMIM}][\text{MS}]$ has already been presented previously.⁴⁸ The PNA analysis of the CH_3 symmetric stretch at the end of the butyl chain showed the tilt angle to be around 53° , and the CH_3 symmetric stretch of the $[\text{MS}]^-$ gave a tilt angle of around 65° .⁴⁸ Unfortunately, for the present work, the tilt angle for the methyl group of the $[\text{EMIM}]^+$ was not calculated, since the peak intensity of the CH_3 symmetric stretch is weak, which may possibly give inaccurate values.

The difference in the preferred orientation of $[\text{MMIM}]^+$, $[\text{EMIM}]^+$, and $[\text{BMIM}]^+$ at the interface may be related to the symmetry of the molecule, as well as the chain interaction. The $[\text{MMIM}]^+$ cation, with a C_{2v} symmetry, is symmetric, whereas for the case of the cation with relatively longer alkyl chains, $[\text{EMIM}]^+$ and $[\text{BMIM}]^+$, this symmetry is broken. In this work, the proposed SFG model for $[\text{EMIM}]^+$ and $[\text{BMIM}]^+$ is similar to the model reported initially by our group for neat ionic liquids based on the $[\text{BMIM}]^+$ cation,^{16,23} in which the imidazolium ring is tilted almost parallel to the surface plane with its butyl chain directed toward the gas phase. This conclusion is in agreement with the molecular dynamics simulations on $[\text{EMIM}][\text{NO}_3]$ by Voth et al.,²⁷ on $[\text{BMIM}][\text{PF}_6]$ by Balasubramanian et al.,²⁹ and on $[\text{BMIM}][\text{PF}_6]$, $[\text{BMIM}][\text{BF}_4]$, and $[\text{BMIM}][\text{Cl}]$ by Del Popolo et al.²⁸ In their simulations, Voth et al.²⁷ discussed their observation of two regions at the surface layer and at the uppermost and the dense regions. A dense region is located right underneath the topmost layer, in which the density is found to be higher than that of the bulk, especially for the cation. In addition, two different cation orientations were observed from both regions. At the topmost layer, the cation has its ring lying parallel to the surface plane, but in the dense region, the ring is

slightly tilted toward the bulk and the ethyl chain is directed toward the vacuum for both models. The suggested SFG model for the cation of the [EMIM][MS] salt resembles the orientation at the topmost layer determined by Voth et al.²⁷ Recent MD simulations on [BMIM][PF₆] exhibit similar features, in which it is ascertained that there are two regions at the surface, and as a result, two kinds of orientation have been depicted in which such preferences were only observed at the first layer. Balasubramanian et al.²⁹ detected that the cation has the tendency to have the ring flat on the surface, whereas the butyl chains orient along the surface normal. This preferential ordering is consistent with the experimental model of SFG. However, underneath this layer, a different orientation has been detected in which the ring is aligned parallel to the surface normal, which seems to be in agreement with the DRS data. The results presented by Del Popolo et al.²⁸ also showed the projection of the butyl chain toward the gas phase, which agrees well with SFG findings.

The SFG results for [EMIM][MS] and [BMIM][MS] salts indicate that the suggested ring orientation for both cations is an average over a distribution of the oriented molecules at the topmost layer and not from the second layer. Molecules beneath the uppermost layer may not be highly oriented enough to be detected by SFG, given that its coherence length is 31 nm.

[EMIM][PF₆]. Conversely, for this particular salt, the [EMIM]⁺ cation orientation deviates from the suggested SFG model for [EMIM][MS] mentioned above. Vibrational modes were observed for both head and tail groups of the cation, as opposed to what were observed in the spectra of [EMIM][MS] and [BMIM]⁺ on the basis of ionic liquids paired with different anions. The presence of the N-CH₃ group and the H-C(4)-C(5)-H of the ring in the SFG spectrum is an indication that the ring could not possibly be lying parallel to the surface plane, as suggested in the preceding discussion for the methylsulfate salts. The ring is considered slightly tilted, with its methyl group directed toward the bulk and the ethyl chain still projecting upward. It is noticed that this analysis fits well with the ring orientation observed by Voth et al.²⁷ in the high-density region of the surface layer in their simulation. It might be important to note that the SFG experiments for [EMIM][MS] and [EMIM][PF₆] were performed at two different temperatures, room temperature and 70 °C, respectively. This could possibly have an influence on the average orientation of the surface molecules. From the simulation, it was deduced that the average number density in the topmost region was lower than the dense region. Hence, a higher temperature could result to a more random environment, giving a relatively random orientation of the surface molecules in comparison with the [EMIM][MS] at room temperature. In this case, the topmost layer could possibly have a higher average orientation of the molecules in which the ring is tilted, showing the vibrational modes of the N-CH₃ group, than when the imidazolium ring is aligned nearly parallel to the surface plane. Alternatively, it could be that the presence of a relatively shorter ethyl chain (compare to the butyl chain) is the factor rather than the temperature. As shown in previous SFG experiments performed at 25 and 80 °C on [BMIM][PF₆], both yielded similar results. The spectra only exhibited vibrational modes from the CH₃ group at the end of the butyl chain, and nothing was observed from the N-CH₃ group or from the ring itself.²³ In addition, the MD simulations of Del Popolo et al.²⁸ on 1-butyl-3-methylimidazolium [PF₆], [BF₄], and [Cl] performed at various temperatures showed that the effects of both temperature and variation with anion on the degree of cation orientation were small. Certainly, the cation of [EMIM]-

[PF₆] has a preferred orientation that differs from the model suggested initially for butylimidazolium-based salts and the [EMIM][MS]. Therefore, the results suggest that the surface orientation of ionic liquids with the shorter ethyl chain could be affected by the anion, as shown in the spectra of [EMIM][MS] and [EMIM][PF₆].

The presence of C-H vibrations from both cation and anion of the methylsulfate salts confirms that both ions are located at the first layer of the surface. This is further supported by the investigation of the surface structure of ionic liquids, for example, [BMIM][PF₆], using X-ray reflectivity measurements. The study shows an increase in the electron density at the surface that arises from the adsorption of the anions to the surface.¹⁵ Conversely, the X-ray reflectivity data do not agree with the two previous independent MD simulations using a similar ionic liquid, [BMIM][PF₆].^{28,29} A very recent study, however, presents factors on the deviation of the simulation results from the experimental data.⁶¹ It was mentioned that differences include the force fields applied and the lack of polarizability employed for the model in the simulations. Although disagreements were found, the qualitative results of the simulations are believed to be correct, particularly the preferential ordering of the cation near the surface and, hence, the associated increased in the density, since both were observed in the two independent simulations.^{28,29} Even the interfacial location of the ions has been verified using SFG and X-ray crystallography, and results for [BMIM][MS] and [BMIM][CH₃SO₃] were presented in a previous paper.⁴⁸ From the study, it is clearly indicated that the ions are located adjacent to one another with the methyl group directed upward, as evident from the crystallographic evidence and phase simulations.⁴⁸

Further investigation of different chain length substituents on both the alkylimidazolium cation and the alkylsulfate anion is currently underway in this laboratory.

Conclusion

SFG spectroscopy has been used to determine the orientation of the ions of room temperature ionic liquids at the gas-liquid interface. The results indicate that both the cation and the anion are present and oriented at the surface. The tilt angles, ~35° and ~65°, of the CH₃ from the dimethylimidazolium ring and the methylsulfate, respectively, have been measured using the more sensitive PNA analysis. The experimental results on the preferred surface orientation of [MMIM]⁺, [EMIM]⁺, and [BMIM]⁺ molecules are in agreement with the molecular dynamics simulation studies of Lynden-Bell,²⁶ Voth et al.,²⁷ and Balasubramanian et al.²⁹

References and Notes

- (1) Wasserscheid, P.; Keim, W. *Angew. Chem., Int. Ed.* **2000**, *39*, 3772-3789.
- (2) Huddleston, J. G.; Willauer, H. D.; Swatoski, R. P.; Visser, A. E.; Rogers, R. D. *Chem. Commun.* **1998**, 1765-1766.
- (3) Welton, T. *Chem. Rev.* **1999**, *99*, 2071-2083.
- (4) Dupont, J.; de Souza, R. F.; Suarez, P. A. Z. *Chem. Rev.* **2002**, *102*, 3667-3692.
- (5) Abraham, M. H.; Zissimos, A. M.; Huddleston, J. G.; Willauer, H. D.; Rogers, R. D.; Acree, W. E. *Ind. Eng. Chem. Res.* **2003**, *42*, 413-418.
- (6) Sheldon, R. *Chem. Commun.* **2001**, 2399-2407.
- (7) Anthony, J. L.; Maginn, E. J.; Brennecke, J. F. *J. Phys. Chem. B* **2002**, *106*, 7315-7320.
- (8) Blanchard, L. A.; Brennecke, J. F. *Ind. Eng. Chem. Res.* **2001**, *40*, 287-292.
- (9) Camper, D.; Scovazzo, P.; Koval, C.; Noble, R. *Ind. Eng. Chem. Res.* **2004**, *43*, 3049-3054.
- (10) Bonhote, P.; Dias, A.; Papageorgiou, N.; Kalyanasundaram, K.; Gratzel, M. *Inorg. Chem.* **1996**, *35*, 1168-1178.

- (11) Mazille, F.; Fei, Z.; Kuang, D.; Zhao, D.; Zakeeruddin, S. M.; Gratzel, M.; Dyson, P. J. *Inorg. Chem.* **2006**, *45*, 1585–1590.
- (12) Wilkes, J. S.; Levisky, J. A.; Wilson, R. A.; Hussey, C. L. *Inorg. Chem.* **1982**, *21*, 1263–1264.
- (13) Quinn, B. M.; Ding, Z.; Moulton, R.; Bard, A. J. *Langmuir* **2002**, *18*, 1734–1742.
- (14) Bowers, J.; Vergara-Gutierrez, M. C. *Langmuir* **2004**, *20*, 309–312.
- (15) Sloutskin, E.; Ocko, B. M.; Tamam, I.; Kuzmenko, I.; Gog, T.; Deutsch, M. *J. Am. Chem. Soc.* **2005**, *127*, 7796–7804.
- (16) Baldelli, S. *J. Phys. Chem. B* **2003**, *107*, 6148–6152.
- (17) Rivera-Rubero, S.; Baldelli, S. *J. Am. Chem. Soc.* **2004**, *126*, 11788–11789.
- (18) Gannon, T. J.; Law, G.; Watson, P. R. *Langmuir* **1999**, *15*, 8429–8434.
- (19) Law, G.; Watson, P. R.; Carmichael, A. J.; Seddon, K. R. *Phys. Chem. Chem. Phys.* **2001**, *3*, 2879–2885.
- (20) Iimori, T.; Iwahashi, T.; Ishii, H.; Seki, K.; Ouchi, Y.; Ozawa, R.; Hamaguchi, H.; Kim, D. *Chem. Phys. Lett.* **2004**, *389*, 321–326.
- (21) Lynden-Bell, R. M.; Kohanoff, J.; Del Popolo, M. G. *Faraday Discuss.* **2005**, *129*, 57–67.
- (22) Del Popolo, M. G.; Lynden-Bell, R. M.; Kohanoff, J. *J. Phys. Chem. B* **2005**, *109*, 5895–5902.
- (23) Rivera-Rubero, S.; Baldelli, S. *J. Phys. Chem. B* **2006**, *110*, 4756–4765.
- (24) Sloutskin, E.; Ocko, B. M.; Taman, I.; Kuzmenko, I.; Gog, T.; Deutsch, M. *J. Am. Chem. Soc.* **2005**, *127*, 7796–7804.
- (25) Rivera-Rubero, S.; Baldelli, S. *J. Phys. Chem. B* **2006**, *110*, 15499–15505.
- (26) Lynden-Bell, R. M. *Mol. Phys.* **2003**, *101*, 2625–2633.
- (27) Yan, T.; Li, S.; Jiang, W.; Gao, X.; Xiang, B.; Voth, G. A. *J. Phys. Chem. B* **2006**, *110*, 1800–1806.
- (28) Lynden-Bell, R. M.; Del Popolo, M. G. *Phys. Chem. Chem. Phys.* **2006**, *8*, 949–954.
- (29) Bhargava, B. L.; Balasubramanian, S. *J. Am. Chem. Soc.* **2006**, *128*, 10073–10078.
- (30) Bain, C. D. *J. Chem. Soc. Faraday Trans.* **1995**, *91*, 1281–1296.
- (31) Buck, M.; Himmelhaus, M. *J. Vac. Sci. Technol. A* **2001**, *19*, 2717–2736.
- (32) Miranda, P. B.; Shen, Y. R. *J. Phys. Chem. B* **1999**, *103*, 3292–3307.
- (33) Shultz, M.; Baldelli, S.; Schnitzer, C.; Simonelli, D. *J. Phys. Chem. B* **2002**, *106*, 5313–5324.
- (34) Gan, W.; Wu, B.; Chen, H.; Guo, Y.; Wang, H.-F. *Chem. Phys. Lett.* **2005**, *406*, 467–473.
- (35) Lu, R.; Gan, W.; Wang, H.-F. *Chin. Sci. Bull.* **2003**, *48*, 2183–2187.
- (36) Lu, R.; Gan, W.; Wu, B.; Zhang, Z.; Guo, Y.; Wang, H.-F. *J. Phys. Chem. B* **2005**, *109*, 14118–14129.
- (37) Holbrey, J. D.; Reichert, W. M.; Swatloski, R. P.; Broker, G. A.; Pitner, W. R.; Seddon, K. R.; Rogers, R. D. *Green Chem.* **2002**, *4*, 407–413.
- (38) Anthony, J. L.; Maginn, E. J.; Brennecke, J. F. *J. Phys. Chem. B* **2001**, *105*, 10942–10949.
- (39) Carter, D. A.; Pemberton, J. E. *J. Raman Spectrosc.* **1997**, *28*, 939–946.
- (40) Romero, C.; Baldelli, S. *J. Phys. Chem. B* **2006**, *110*, 6213–6223.
- (41) MacPhail, R. A.; Strauss, H. L.; Snyder, R. G. *J. Phys. Chem.* **1984**, *88*, 334–341.
- (42) Stanners, C. D.; Du, Q.; Chin, R. P.; Cremer, P.; Somorjai, G. A.; Shen, Y.-R. *Chem. Phys. Lett.* **1995**, *232*, 407–413.
- (43) Ma, G.; Allen, H. C. *J. Phys. Chem. B* **2003**, *107*, 6343–6349.
- (44) Superfine, R.; Huang, J. Y.; Shen, Y. R. *Phys. Rev. Lett.* **1991**, *66*, 1066–1069.
- (45) Chang, H.-C.; Jiang, J.-C.; Tsai, W.-C.; Chen, G.-C.; Lin, S. H. *J. Phys. Chem. B* **2006**, *110*, 3302–3307.
- (46) Talaty, E. R.; Raja, S.; Storhaug, V. J.; Dolle, A.; Carper, W. R. *J. Phys. Chem. B* **2004**, *108*, 13177–13184.
- (47) Bain, C. D. *J. Chem. Soc. Faraday Trans.* **1995**, *91*, 1281.
- (48) Santos, C.; Rivera-Rubero, S.; Dibrov, S.; Baldelli, S. *J. Phys. Chem. B* **2006**, Submitted.
- (49) Wang, H.-F.; Gan, W.; Lu, R.; Rao, Y.; Wu, B. H. *Int. Rev. Phys. Chem.* **2005**, *24*, 191.
- (50) Bain, C. D.; Davies, P. B.; Ong, T. H.; Ward, R. N. *Langmuir* **1991**, *7*, 1563.
- (51) Bell, G. R.; Li, Z. X.; Bain, C. D.; Fischer, P.; Duffy, D. C. *J. Phys. Chem. B* **1998**, *102*, 9461.
- (52) Hirose, C.; Yamamoto, H.; Akamatsu, N.; Domen, K. *J. Phys. Chem.* **1993**, *97*, 10064.
- (53) Hirose, C.; Akamatsu, N.; Domen, K. *J. Chem. Phys.* **1992**, *96*, 997.
- (54) Hirose, C.; Akamatsu, N.; Domen, K. *Appl. Spectrosc.* **1992**, *46*, 1051.
- (55) Sung, J.; Jeon, Y.; Kim, D.; Iwahashi, T.; Iimori, T.; Seki, K.; Ouchi, Y. *Chem. Phys. Lett.* **2005**, *406*, 495–500.
- (56) Langmuir, I. *Trans. Faraday Soc.* **1920**, *15*, 62–74.
- (57) Adamson, A. W.; Gast, A. P. *Physical Chemistry of Surfaces*; 6th ed.; John Wiley & Sons, Inc.: New York, 1997.
- (58) Langmuir, I. *Chem. Metall. Eng.* **1916**, 468–470.
- (59) Smith, E. F.; Garcia, I. J.; Briggs, D.; Licence, P. *Chem. Commun.* **2005**, 5633–5635.
- (60) Smith, E. F.; Rutten, F. J. M.; Villar-Garcia, I. J.; Briggs, D.; Licence, P. *Langmuir* **2006**, *22*, 9386–9392.
- (61) Sloutskin, E.; Lynden-Bell, R. M.; Balasubramanian, S.; Deutsch, M. *J. Chem. Phys.* **2006**.